NANO LETTERS

LETTER

pubs.acs.org/NanoLett

Graphene Veils and Sandwiches

Jong Min Yuk,[†,‡,∥] Kwanpyo Kim,[‡,∥] Benjamín Alemán,[‡,∥] William Regan,[‡,∥] Ji Hoon Ryu,[†] Jungwon Park,[§,∥] Peter Ercius,[⊥] Hyuck Mo Lee,[†] A. Paul Alivisatos,[§,∥] Michael F. Crommie,[‡,∥] Jeong Yong Lee,[*,†] and Alex Zettl[*,‡,∥]

[†]Department of Materials Science and Engineering, KAIST, Daejeon 305-701, Korea

[‡]Department of Physics and Center of Integrated Nanomechanical Systems and [§]Department of Chemistry, University of California at Berkeley, California 94720, United States

[∥]Materials Sciences Division and [⊥]National Center for Electron Microscopy, Lawrence Berkeley National Laboratory, Berkeley, California 94720, United States

Supporting Information

ABSTRACT: We report a new and highly versatile approach to artificial layered materials synthesis which borrows concepts of molecular beam epitaxy, self-assembly, and graphite intercalation compounds. It readily yields stacks of graphene (or other two-dimensional sheets) separated by virtually any kind of "guest" species. The new material can be "sandwich like", for which the guest species are relatively closely spaced and form a near-continuous inner layer of the sandwich, or "veil like", where the guest species are widely separated, with each guest individually draped within a close-fitting, protective yet atomically thin graphene net or veil. The veils and sandwiches can be intermixed and used as a two-dimensional platform to control the movements and chemical interactions of guest species.

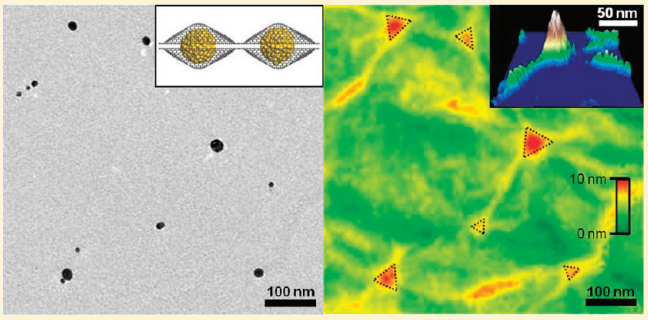

KEYWORDS: Graphene, stacks of graphene, two-dimensional sheets, artificial layered materials, two-dimensional platform

The development of molecular beam epitaxy (MBE)[1,2] in the late 1960s and early 1970s heralded a new era in materials synthesis whereby structures unattainable by conventional crystal growth methods could be produced artificially, virtually atom-by-atom. Despite the phenomenal scientific success of MBE, the method is technically intensive and has many limitations. Another approach toward tailored layered materials is solution-based self-assembly,[3,4] where appropriate surface chemistry is used to coax desired sequential and easily patterned molecular attachment. Graphite intercalation compounds (GICs),[5,6] produced by allowing selected atoms or molecules to naturally insert themselves between the graphene layers of graphite crystals, might also be viewed as a primitive form of self-assembly. Concepts of these methods can be adapted to combine various functional materials with two-dimensional (2D) atomic-thick crystals, such as graphene, boron nitride (BN), several dichalcogenides, and complex oxides, exhibiting dramatically different properties with their 3D bulk materials.[7]

Our approach to custom engineered layered compounds utilizes thin preformed "host" sheets of materials which are sequentially stacked, layer-by-layer.[8−10] Prior to the placement of each new sheet, however, "guest" species can be deposited on the surface of the previous sheet. The guest deposition can be achieved via evaporation, sputtering methods, or solution deposition. Unlike the case for intercalation approaches, here the guest species are virtually unrestricted.[5,6]

In the study reported here, we employ graphene as a prototypical host material[11,12] and metallic and semiconducting nanocrystals and nanorods as prototypical guest species. Of course, other hosts and guests are possible, including layered dichalcogenides or BN (or combinations)[7] as hosts and alkali metals, organic complexes, and thin metal or dielectric films as guests. Graphene is a particularly desirable host, since it is atomically thin with few defects[13] and displays extraordinary electrical, mechanical, and thermal properties.[14−16]

To produce graphene veil or sandwich superstructures, we start with large-area single-layer graphene (SLG) grown by chemical vapor deposition[17] and transfer it to arbitrary rigid substrates such as SiO_2, Si, or mica (Figure 1a). Quasi-free-standing superstructures are also produced for transmission electron microscopy (TEM) characterization utilizing Quantifoil TEM grids. Guest species selected from Au, Pd, Sn, Co, and PbSe are deposited onto the graphene layer by drop-casting chemically synthesized nanoparticles or by electron (e)-beam evaporation (Figure 1b). A second single-layer graphene (SLG) sheet is transferred onto the first decorated graphene sheet thus covering the predeposited materials (Figure 1c). To prevent folding or tearing of the second graphene layer, the transfer process requires

Received: May 16, 2011
Revised: July 1, 2011
Published: July 19, 2011

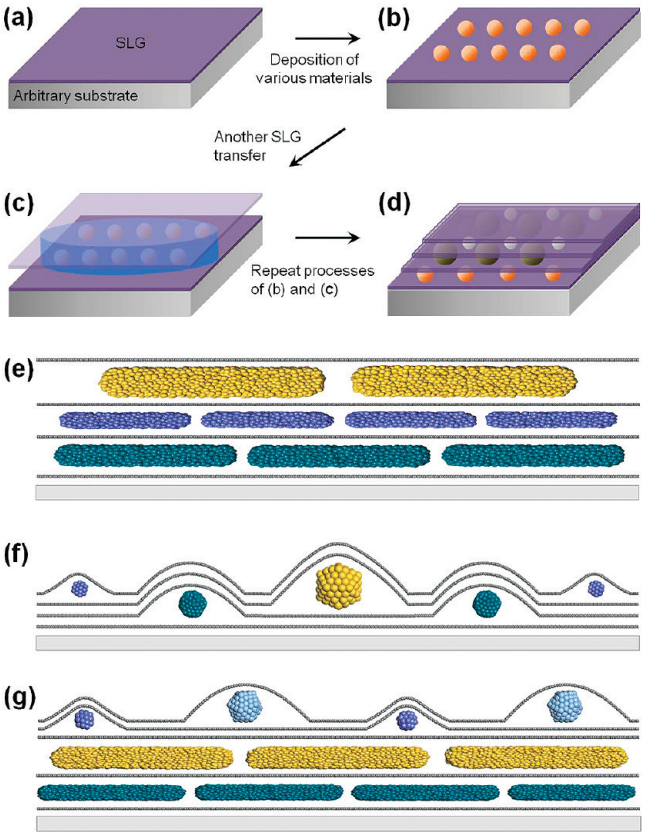

Figure 1. Schematic of the process flow for graphene-based superstructure fabrication. (a) Large-area SLG on an arbitrary substrate. (b) Deposition of various materials by either drop-casting chemically synthesized materials or e-beam evaporation. (c) A second SLG is superimposed on the first graphene layer, thus encapsulating the deposited materials. IPA is used to wet the graphene layers and intercalants to improve graphene−graphene or graphene−intercalant bonding after drying. (d) Repeating steps b and c results in a multilayer graphene-based superstructure encapsulating different materials. (e−g) Schematics of a graphene sandwich superstructure (GSS), graphene veil superstructure (GVS), and a hybrid superstructure of GSSs and GVSs. Various types of intercalants are represented by different colors and sizes.

a rigid support such as the holey amorphous carbon film of a Quantifoil TEM grid or a polymethyl methacrylate polymer backing. Isopropanol (IPA) is used to wet both graphene layers, and as the IPA evaporates surface tension pulls the graphene layers together to form a physical seal. If desired, the rigid support structure can be removed after the IPA fully evaporates.[18,19] For higher-layer veil or sandwich structures, the guest deposition and graphene layer addition processes are repeated (Figure 1d).

The coupling between graphene layers and encapsulated materials is easily tuned by controlling the density and packing structure of the guest material during deposition. For high densities or large sizes of guest species, adjacent graphene layers have little chance to seal together in the region between guests; hence, the possibility exists for guest species motion between the graphene layers or atom exchange between guests. We term this structure a graphene sandwich superstructure (GSS) (Figure 1e). In the case of singular or more isolated guests, the guests are effectively laminated between adjacent graphene sheets (or between graphene and the original substrate, if desired). We term this configuration a graphene veil superstructure (GVS) (Figure 1f). The distinct GSS and GVS morphologies can be sequentially combined to create hybrid superstructures as shown in Figure 1g.

We initially examine the structural morphology of a GVS containing only chemically synthesized Au nanoparticles with ∼10−24 nm diameters. We measure the size of the encapsulated particles and topography of the superstructure surface by TEM and atomic force microscopy (AFM) (Figure 2a,b). Embedded particles induce relatively sharp local protrusions in the host graphene layers. We find that individual graphene veils encapsulating spherical Au nanoparticles often have a triangular pyramidal shape with associated ridges or wrinkles extending from the apex in three directions, which likely reflects the lattice symmetry (C_{3v}) of graphene.[20] Nanoparticles are encapsulated in the ridges or along the wrinkles. The deviation angle from the horizontal plane in the graphene veil (∼21°, inset of Figure 2b) is larger than the deviation angle (∼5°) of normal suspended graphene.[21] The width (w) of a graphene veil is approximately proportional to the radius (R) of the encapsulated particle and is larger than the diameter of the encapsulated particle (Figure 2c).

The relation between w and R can be understood by considering the surface tension (T) and attractive van der Waals energy ($E_v \sim 0.3$ J/m^2) between graphene sheets.[22] Figure 2d shows a simple two-dimensional model of a graphene veil structure with the width w around the encapsulated particle. Outside of the veil structure, the double layer graphene is bonded via the van der Waals interaction. Graphene layers in the veil structure are decoupled from each other at clamped points with an angle θ, the deviation angle of the graphene from the horizontal plane. From these geometrical considerations, the relation between w and R can be written as $w = 2R/\sin\theta$. By considering the force components in the y-direction at each clamped point, T in the graphene layer can be estimated as $T \sin\theta \sim E_v$. Therefore, we have the following relation between w and R:

$$w \sim \frac{2T}{E_v} R$$

According to our model, w will be proportional to R at a certain constant value of T, which agrees well with our experimental data (Figure 2c). The assumption of the constant tension T in graphene is also reasonable, since T mainly depends on the method of the graphene veil preparation.[23,24] The slope of the fitting line from data in Figure 2c yields $\theta \sim 21°$ and $T \sim 0.8$ N/m for our graphene veil structures.

For a given graphene structure encapsulating nanoparticles with an average size R, the distinct veil structure becomes blurred when $w(R)$ is equal to $\tilde{d}$, the average distance between particles. When the average distance between particles is larger than the width of the graphene veil ($\tilde{d} > w$), individual particles are mainly isolated from each other resulting in a well-defined GVS. In the case of $\tilde{d} < w$, open graphene channels are created between guest particles, resulting in an effective GSS.

Even if the same host material (graphene) and guest species are employed, the physical properties of unveiled, veil, and sandwich structures can be remarkably different. Here we examine the high temperature behavior of Au nanoparticles on open (unveiled) SLG, in a GVS, and in a GSS. We perform in situ TEM Joule heating experiments[25] and examine the evolution of the Au particles in real time. Figure 3a shows two frames from a

dx.doi.org/10.1021/nl201647p |Nano Lett. 2011, 11, 3290–3294

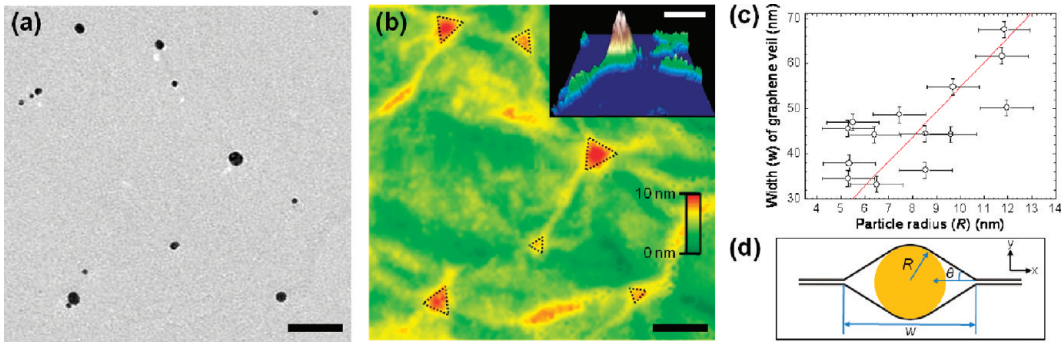

Figure 2. Complementary TEM and AFM images of GVS and the relation between the width of a graphene veil and the radius of encapsulated particle: (a) TEM image of a suspended GVS encapsulating particle ~10−24 nm in diameter. (b) AFM image of the GVS corresponding to part a. Scale bars represent 100 nm. (Inset) Three-dimensional topographical map of a graphene veil with a triangular pyramid shape and associated wrinkles (max height = 6 nm, and the scale bar represents 50 nm). (c) Width (w) of graphene veils versus particle radius (R). The experimental data are fit by a linear function shown as a straight line. (d) Two-dimensional model of graphene veil structure. The yellow circle and black line represent an encapsulated particle and graphene layers, respectively.

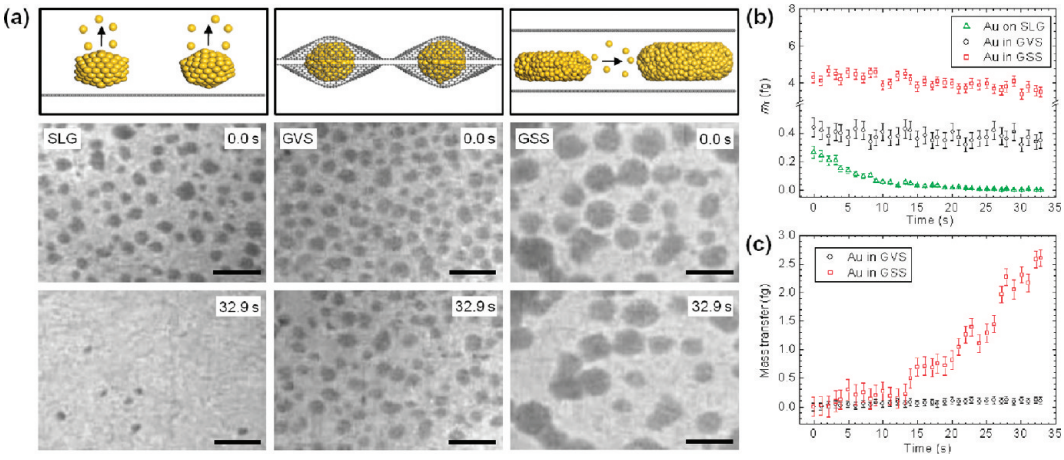

Figure 3. In situ TEM Joule heating experiment of Au nanoparticles on a SLG, in a GVS, and in a GSS. (a) Two frames from a video sequence acquired 32.9 s apart of Au nanoparticles at their melting temperature on a SLG, in a GVS, and in a GSS. Top schematics show cross-sectional views of the corresponding TEM images, respectively. Scale bars represent 50 nm. (b) Total mass (m_T) of particles versus Joule heating time. (c) Mass transfer versus Joule heating time.

video sequence, acquired 32.9 s apart, of Au nanoparticles at their melting temperature of approximately 1300 K.[26] In general, the particles are nearly round and exhibit dark TEM contrast independent of their orientation and size, which indicates that they are molten. During the in situ Joule heating experiment, we track $m_i(t)$, the mass of the ith particle at Joule heating time t. We approximate particles as cylinders with diameters ~5 times the height.[27] The mass of the particle can be calculated by $(19.3\ \mathrm{g\ cm^{-3}})(\pi(D/2)^2)(D/5)$, where the diameter ($D$) of each particle is measured from video frames (Movies S1 and S2 in the Supporting Information). Figure 3b shows the total mass of particles, $m_T = \Sigma_i m_i(t)$ on a SLG, in a GVS, and in a GSS as a function of the Joule heating time. The m_T for particles on the SLG decays exponentially with time because Au nanoparticles evaporate almost immediately upon reaching their melting temperature due to their high vapor pressure (2.17×10^{-3} Pa)[28] relative to the TEM vacuum ($<10^{-5}$ Pa). However, in the GVS and GSS cases, over 80% of the particles' mass remains even after a heating time sufficient to evaporate all particles on a SLG. The graphene membranes appear to protect the encapsulated nanoparticles from free evaporation (Movies S1 and S2 in the Supporting Information).[23,29,30] It is likely that the missing 20% of particle mass for GVS and GSS configurations is due to migration out of the imaged region or limited evaporation through openings in the graphene layers.

To understand the interaction between Au particles, we examine the real time mass transfer, $\Sigma_i|m_i(t) - m_i(0)|$ in a GVS and GSS as shown in Figure 3c. This parameter considers not only net mass loss from the system but also mass exchange between particles. For Au in a GVS, the mass transfer is approximately 20% of the total mass after 32.9 s, which is very close to the total mass loss in a GVS. This indicates that Au particles in GVS do not exchange their masses; the encapsulating graphene sheets prohibit migration and agglomeration of particles. The GVS physically confines and stabilizes encapsulated liquid materials at high temperature, sealing the sparse guest species in graphene pockets with surrounding regions of double-layer graphene (Movie S3 in the Supporting Information).[23,29,30] This is clearly different than the behavior of carbon coated nanoparticles at high temperature or under an intense electron

dx.doi.org/10.1021/nl201647p |Nano Lett. 2011, 11, 3290–3294

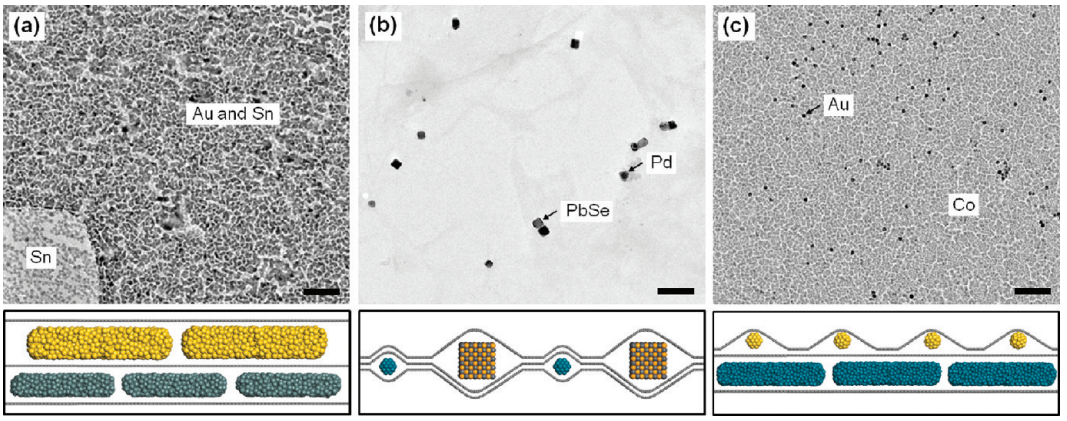

Figure 4. TEM images of GSS, GVS, and a hybrid of the two superstructures: (a) GSS encapsulating metallic materials (Sn and Au), (b) GVS encapsulating metallic (Pd) and semiconducting (PbSe) materials, (c) hybrid superstructure of GSS and GVS encapsulating magnetic (Co) and metallic (Au) materials, respectively. Below each image, schematics show cross-sectional views of the corresponding TEM images. Scale bars represent 100 nm.

beam, in which they coalescence via rupture of the passivating carbon shell.[31] Although local stretching of the graphene−graphene distance along the out of plane direction occurs near guest particles, other areas without nanoparticles are perfectly coupled and produce Moiré patterns (Figure S1 in the Supporting Information).[32] The Moiré pattern depends on the in-plane rotation between the hexagonal lattices of the upper and lower graphene layers (Figure S2 in the Supporting Information). The misalignments observed in our artificial graphene superstructures are clearly different from naturally occurring bilayer graphene with Bernal (AB) stacking of graphite and the AAA... stacking of carbon nanofilms.[33] In a GSS, the mass transfer is approximately 60% of the total mass after 32.9 s, more than 3 times the total mass loss. This behavior is starkly different than that for a GVS. Particles in a GSS can migrate and agglomerate together. In the case of Au nanoparticles described here, the mass transport is apparently via single-atom migration in the relatively "open" region between slightly separated graphene sheets.[34]

In principle, there is no limit to the number of graphene transfer and deposition steps used in fabrication of a given graphene superstructure, which allows the fabrication of virtually any desirable structure. The number of graphene layers between different guest species can be also precisely controlled by the number of subsequent SLG transfer steps. There are a variety of materials that can be incorporated into the superstructure. We have examined conducting guests (for example, Au, Pd, and Sn), semiconducting guests (PbSe), and magnetic guests (Co).

Figure 4 shows higher-order graphene-based veil, sandwich, and hybrid veil/sandwich structures built up from multiple deposition steps and using a variety of guests. The morphology of the guests and the number of SLGs separating guests are confirmed by selected-area electron diffraction patterns (Figure S3 in the Supporting Information). Figure 4a shows multilayer GSS (SLG/Sn/SLG/Au/SLG), fabricated by deposition of Sn and Au with nominal thicknesses of ∼3 and ∼5 nm on the graphene by e-beam evaporation. Graphene is generally chemically inert, causing the guests to form metal islands rather than wetting the graphene surface.[35] In the case of e-beam evaporated nanoparticles, grain boundaries, and some bilayer or multilayer regions of graphene could influence nanoparticle adhesion on SLG.[27,36] However, nanoparticle adhesion in GSSs and GVSs seems to be more affected by the ridges or wrinkles of graphene sheets, which make nanoparticles array or come together in GSSs (Figure S4 in the Supporting Information). Figure 4b shows multilayer GVS (SLG/Pd/SLG/PbSe/SLG), fabricated by drop-casting chemically synthesized Pd and PbSe with average diameters of ∼15 and ∼20 nm on the graphene. Encapsulation of particles can result in GVSs with folded and wrinkled graphene structures. Figure 4c shows multilayer hybrid superstructure of GSS and GVS (SLG/Co/SLG/Au/SLG), fabricated by deposition of Co with nominal thickness of ∼4 nm followed by drop-casting chemically synthesized Au particles with average diameters of ∼7 nm on the graphene.

These veil, sandwich, and hybrid superstructures can be used as nanoscale reaction chambers for alloying and coalescence of diverse guest materials. In addition, the veils and sandwiches, which can be intermixed, have implications for chemical sensors, solar cells, batteries, and other optical, magnetic, and structural applications.

■ ASSOCIATED CONTENT

Ⓢ Supporting Information. Graphene sample preparation, preparation of nanocrystals, graphene sandwich superstructure and graphene veil superstructure fabrication, TEM and AFM imaging processing, supporting Figures S1−S4, and supporting Movies S1−S3. This material is available free of charge via the Internet at http://pubs.acs.org.

■ AUTHOR INFORMATION

Corresponding Author
*E-mail: j.y.lee@kaist.ac.kr (J.Y.L.); azettl@berkeley.edu (A.Z.).

■ ACKNOWLEDGMENT

We thank W. Gannett for helpful discussions and M. L. Tang at U.C. Berkeley for helpful discussions and for preparation of nanoparticles. This research was supported in part by the Director, Office of Energy Research, Materials Sciences and Engineering Division, of the U.S. Department of Energy under Contract No. DE-AC02-05CH11231, which provided for in situ TEM experiments; by the National Science Foundation within the Center of Integrated Nanomechanical Systems, under Grant EEC-0832819, which provided for CVD graphene synthesis; by

the Physical Chemistry of Semiconductor Nanocrystals Program, KC3105, Director, Office of Science, Office of Basic Energy Sciences, of the United States Department of Energy under Contract DE-AC02-05CH11231, which provided for nanoparticle synthesis; and by the National Science Foundation under Grant No. 0906539, which provided for design of the experiment, sample preparation, and analysis of the results. High-resolution imaging of graphene was performed at the National Center for Electron Microscopy, Lawrence Berkeley National Laboratory, which is supported by the U.S. Department of Energy under Contract No. DE-AC02-05CH11231. J.M.Y. and J.Y.L. acknowledge the financial support from Priority Research Centers Program through the National Research Foundation of Korea (NRF) funded by the Ministry of Education, Science and Technology (Grant No. 2009-0094040); W.R. acknowledges support through a National Science Foundation Graduate Research Fellowship; and B.A. acknowledges support from the UC Berkeley A.J. Macchi Fellowship Fund in the Physical Sciences.

REFERENCES

(1) Panish, M. B. Molecular Beam Epitaxy. *Science* **1980**, *208*, 916–922.

(2) Arthur, J. R. Molecular beam epitaxy. *Surf. Sci.* **2002**, *500*, 189–217.

(3) Colvin, V. L.; Goldstein, A. N.; Alivisatos, A. P. Semiconductor Nanocrystals Covalently Bound to Metal-Surfaces with Self-Assembled Monolayers. *J. Am. Chem. Soc.* **1992**, *114*, 5221–5230.

(4) Rabani, E.; Reichman, D. R.; Geissler, P. L.; Brus, L. E. Drying-mediated self-assembly of nanoparticles. *Nature* **2003**, *426*, 271–274.

(5) Zabel, H.; Solin, S. A. *Graphite Intercalation Compounds I*; Springer: Berlin, Germany, 1990. Zabel, H.; Solin, S. A. *Graphite Intercalation Compounds II*; Springer: Berlin, Germany, 1992.

(6) Dresselhaus, M. S.; Dresselhaus, G. Intercalation compounds of graphite. *Adv. Phys.* **2002**, *51*, 1–186.

(7) Novoselov, K. S.; Jiang, D.; Schedin, F.; Booth, T. J.; Khotkevich, V. V.; Morozov, S. V.; Geim, A. K. Two-dimensional atomic crystals. *Proc. Natl. Acad. Sci. U.S.A.* **2005**, *102*, 10451–10453.

(8) Bae, S.; Kim, H.; Lee, Y.; Xu, X.; Park, J.-S.; Zheng, Y.; Balakrishnan, J.; Lei, T.; Kim, H. R.; Song, Y. I.; Kim, Y.-J.; Kim, K. S.; Özyilmaz, B.; Ahn, J.-H.; Hong, B. H.; Iijima, S. Roll-to-roll production of 30-in. graphene films for transparent electrodes. *Nat. Nanotechnol.* **2010**, *5*, 574–578.

(9) Dean, C. R.; Young, A. F.; Meric, I.; Lee, C.; Wang, L.; Sorgenfrei, S.; Watanabe, K.; Taniguchi, T.; Kim, P.; Shepard, K. L.; Hone, J. Boron nitride substrates for high-quality graphene electronics. *Nat. Nanotechnol.* **2010**, *5*, 722–726.

(10) Unarunotai, S.; Koepke, J. C.; Tsai, C.-L.; Du, F.; Chialvo, C. E.; Murata, Y.; Haasch, R.; Petrov, I.; Mason, N.; Shim, M.; Lyding, J.; Rogers, J. A. Layer-by-Layer Transfer of Multiple, Large Area Sheets of Graphene Grown in Multilayer Stacks on a Single SiC Wafer. *ACS Nano* **2010**, *4*, 5591–5598.

(11) Stankovich, S.; Dikin, D. A.; Dommett, G. H. B.; Kohlhaas, K. M.; Zimney, E. J.; Stach, E. A.; Piner, R. D.; Nguyen, S. T.; Ruoff, R. S. Graphene-based composite materials. *Nature* **2006**, *442*, 282–286.

(12) Kim, N.; Kim, K. S.; Jung, N.; Brus, L.; Kim, P. Synthesis and Electrical Characterization of Magnetic Bilayer Graphene Intercalate. *Nano Lett.* **2011**, *11*, 860–865.

(13) Meyer, J. C.; Kisielowski, C.; Erni, R.; Rossell, M. D.; Crommie, M. F.; Zettl, A. Direct Imaging of Lattice Atoms and Topological Defects in Graphene Membranes. *Nano Lett.* **2008**, *8*, 3582–3586.

(14) Castro Neto, A. H.; Guinea, F.; Peres, N. M. R.; Novoselov, K. S.; Geim, A. K. The electrical properties of graphene. *Rev. Mod. Phys.* **2009**, *81*, 109–162.

(15) Lee, C.; Wei, X.; Kysar, J. W.; Hone, J. Measurement of the Elastic Properties and Intrinsic Strength of Monolayer Graphene. *Science* **2008**, *321*, 385–388.

(16) Baladin, A. A.; Ghosh, S.; Bao, W.; Calizo, I.; Teweldebrhan, D.; Miao, F.; Lau, C. N. Superior Thermal Conductivity of Single-Layer Graphene. *Nano Lett.* **2008**, *8*, 902–907.

(17) Li, X.; Cai, W.; An, J.; Kim, S.; Nah, J.; Yang, D.; Piner, R.; Velamakanni, A.; Jung, I.; Tutuc, E.; Banerjee, S. K.; Colombo, L.; Ruoff, R. S. Large-Area Synthesis of High-Quality and Uniform Graphene Films on Copper Foils. *Science* **2009**, *324*, 1312–1314.

(18) Regan, W.; Alem, N.; Alemán, B.; Geng, B.; Girit, Ç.; Maserati, L.; Wang, F.; Crommie, M.; Zettl, A. A Direct Transfer of Layer-Area Graphene. *Appl. Phys. Lett.* **2010**, *96*, 113102.

(19) Reina, A.; Son, H.; Jiao, L.; Fan, B.; Dresselhaus, M. S.; Liu, Z.; Kong, J. Transferring and Identification of Single- and Few-Layer Graphene on Arbitrary Substrates. *J. Phys. Chem. C* **2008**, *112*, 17741–17744.

(20) Levy, N.; Burke, S. A.; Meaker, K. L.; Panlasigui, M.; Zettl, A.; Guinea, F.; Castro Neto, A. H.; Crommie, M. F. Strain-Induced Pseudo−Magnetic Fields Greater Than 300 T in Graphene Nanobubbles. *Science* **2010**, *329*, 544–547.

(21) Meyer, J. C.; Geim, A. K.; Katsnelson, M. I.; Novoselov, K. S.; Booth, T. J.; Roth, S. The Structure of Suspended Graphene Sheets. *Nature* **2007**, *446*, 60–63.

(22) Chopra, N. G.; Benedict, L. X.; Crespi, V. H.; Cohen, M. L.; Louie, S. G.; Zettl, A. Fully collapsed carbon nanotubes. *Nature* **1995**, *377*, 135–138.

(23) Bunch, J. S.; Verbridge, S. S.; Alden, J. S.; van der Zande, A. M.; Parpia, J. M.; Craighead, H. G.; McEuen, P. L. Impermeable Atomic Membranes from Graphene Sheets. *Nano Lett.* **2008**, *8*, 2458–2462.

(24) Bunch, J. S.; van der Zande, A. M.; Verbridge, S. S.; Frank, I. W.; Tanenbaum, D. M.; Parpia, J. M.; Craighead, H. G.; McEuen, P. L. Electromechanical Resonators from Graphene Sheets. *Science* **2007**, *315*, 490–493.

(25) Kim, K.; Regan, W.; Geng, B.; Alemán, B.; Kessler, B. M.; Wang, F.; Crommie, M. F.; Zettl, A. High-temperature stability of suspended single-layer graphene. *Phys. Status Solidi (RRL)* **2010**, *4*, 302–304.

(26) Koga, K.; Ikeshoji, T.; Sugawara, K. I. Size- and Temperature-Dependent Structural Transitions in Gold Nanoparticles. *Phys. Rev. Lett.* **2004**, *92*, 115507.

(27) Luo, Z.; Somers, L. A.; Dan, Y.; Ly, T.; Kybert, N. J.; Mele, E. J. Charlie Johnson, A. T. Size-Selective Nanoparticle Growth on Few-Layer Graphene Films. *Nano Lett.* **2010**, *10*, 777–781.

(28) Kazenas, E. K.; Astakhova, G. K. Vapor Pressure of Metals. *Russian Metallurgy (Metally)* **1997**, No. 2, 15–35.

(29) Stolyarova, E.; Stolyarov, D.; Bolotin, K.; Ryu, S.; Liu, L.; Rim, K. T.; Klima, M.; Hybertsen, M.; Pogorelsky, I.; Pavlishin, I.; Kusche, K.; Hone, J.; Kim, P.; Stormer, H. L.; Yakimenko, V.; Flynn, G. Observation of Graphene Bubbles and Effective Mass Transport under Graphene Films. *Nano Lett.* **2009**, *9*, 332–337.

(30) Garaj, S.; Hubbard, W.; Reina, A.; Kong, J.; Branton, D.; Golovchenko, J. A. Graphene as a subnanometre trans-electrode membrane. *Nature* **2010**, *467*, 190–193.

(31) Sutter, E.; Sutter, P.; Zhu, Y. Assembly and Interaction of Au/C Core-Shell Nanostructures: In Situ Observation in the Transmission Electron Microscope. *Nano Lett.* **2005**, *5*, 2092–2096.

(32) Warner, J. H.; Rümmeli, M. H.; Gemming, T.; Büchner, B.; Briggs, G. A. D. Direct Imaging of Rotational Stacking Faults in Few Layer Graphene. *Nano Lett.* **2009**, *9*, 102–106.

(33) Horiuchi, S.; Gotou, T.; Fujiwara, M.; Sotoaka, R.; Hirata, M.; Kimoto, K.; Asaka, T.; Yokosawa, T.; Matsui, Y.; Watanabe, K.; Sekita, M. Carbon Nanofilm with a New Structure and Property. *Jpn. J. Appl. Phys.* **2003**, *42*, L1073–L1076.

(34) Jin, Z.; Nackashi, D.; Lu, W.; Kittrell, C.; Tour, J. M. Decoration, Migration, and Aggregation of Palladium Nanoparticles on Graphene Sheets. *Chem. Mater.* **2010**, *22*, 5695–5699.

(35) Bardotti, L.; Tournus, F.; Mélinon, P.; Pellarin, M.; Broyer, M. Mass-selected clusters deposited on graphite: Spontaneous organization controlled by cluster surface reaction. *Phys. Rev. B* **2011**, *83*, 035425.

(36) Zhou, H.; Qiu, C.; Liu, Z.; Yang, H.; Hu, L.; Liu., J.; Yang, H.; Gu, C.; Sun, L. Thickness-Dependent Morphologies of Gold on *N*-Layer Graphenes. *J. Am. Chem. Soc.* **2010**, *132*, 944–946.